Implications for the hydrologic cycle under climate change due to the expansion of bioenergy crops in the Midwestern United States

Phong V. V. Le[a], Praveen Kumar[a,1], and Darren T. Drewry[b]

[a]Department of Civil and Environmental Engineering, University of Illinois, Urbana, IL 61801; and [b]Max-Planck-Institut für Biogeochemie, Postfach 100164, D-07701 Jena, Germany

Edited by Ignacio Rodriguez-Iturbe, Princeton University, Princeton, NJ, and approved August 3, 2011 (received for review May 8, 2011)

To meet emerging bioenergy demands, significant areas of the large-scale agricultural landscape of the Midwestern United States could be converted to second generation bioenergy crops such as miscanthus and switchgrass. The high biomass productivity of bioenergy crops in a longer growing season linked tightly to water use highlight the potential for significant impact on the hydrologic cycle in the region. This issue is further exacerbated by the uncertainty in the response of the vegetation under elevated CO_2 and temperature. We use a mechanistic multilayer canopy-root-soil model to (*i*) capture the eco-physiological acclimations of bioenergy crops under climate change, and (*ii*) predict how hydrologic fluxes are likely to be altered from their current magnitudes. Observed data and Monte Carlo simulations of weather for recent past and future scenarios are used to characterize the variability range of the predictions. Under present weather conditions, miscanthus and switchgrass utilized more water than maize for total seasonal evapotranspiration by approximately 58% and 36%, respectively. Projected higher concentrations of atmospheric CO_2 (550 ppm) is likely to decrease water used for evapotranspiration of miscanthus, switchgrass, and maize by 12%, 10%, and 11%, respectively. However, when climate change with projected increases in air temperature and reduced summer rainfall are also considered, there is a net increase in evapotranspiration for all crops, leading to significant reduction in soil-moisture storage and specific surface runoff. These results highlight the critical role of the warming climate in potentially altering the water cycle in the region under extensive conversion of existing maize cropping to support bioenergy demand.

Rapidly growing energy demand, worldwide depletion of fossil fuels, and global warming are raising an interest in expanding clean and renewable bioenergy production. In the United States, the current starch-based bioethanol production only contributes a small portion of total energy needs (1, 2), but it is raising new challenges related to environmental issues (3–6) and a competition with food production on available fertile land (7). Bioenergy extracted from lignocellulosic feedstocks offers the possible use of marginal land (8), along with many energy, environmental, and economic advantages over current biofuel sources (9), and is being considered as a promising alternative to sustainably meet the US Department of Energy target for bioenenergy and biobased products in the future (10). At present, *Miscanthus × giganteus* (miscanthus) and *Panicum virgatum* (switchgrass) are considered as the two perennial grasses with the highest potential for lignocellulosic bioenergy production in the Midwest with high biofuels yield per unit land area, reduced requirement of nutrient inputs (11, 12), and low net CO_2 emissions (13–16). However, if large portions of the landscape in the Midwestern United States are converted to these crops for meeting bioenergy demands, for example, by using land that supports maize production, it is likely to significantly impact the hydrologic cycle.

A number of studies have been conducted to compare the water use associated with bioenergy crop production in the Midwest. Much of this work has estimated that the total evapotranspiration (*ET*) of miscanthus and switchgrass is higher relative to that of maize using methods such as the residual energy balance method (17), water budget estimation (18), and model-based approaches (19). Each of these studies highlighted the role of higher leaf area index (*LAI*) and longer growing season as the primary reason for the increase, but estimates of water use increase vary considerably. For instance, Hickman, et al (17) estimated that miscanthus and switchgrass increase total growing season *ET* by 343 and 153 mm relative to maize, respectively, while McIsaac, et al (18) showed that miscanthus increases total *ET* by 104 mm relative to maize, with switchgrass and maize having comparable total *ET*.

The present work evaluates potential impacts of biofuel-based land use changes on the hydrologic cycle through simultaneous considerations of (*i*) above-ground canopy structure and function as a result of changes in crop type and (*ii*) vegetation response to climate change as manifested through elevated atmospheric CO_2, higher temperature, and altered precipitation magnitude. Land use conversion from maize to bioenergy crops significantly modifies above-ground canopy structure, affecting near-surface hydrological processes in several ways. Higher *LAI* allows these perennial crops to intercept more rainfall before reaching the soil, which is then lost through evaporation, in combination with evaporative losses of increased condensation moisture on leaf surfaces (20, 21). Denser foliage will also modify the canopy radiative regime and within-canopy micro-climate (22), impacting *ET*, for example, by way of reduced soil evaporation as a result of the reduced energy flux reaching the ground surface (23). While alterations in canopy structure affect energy and water partitioning above ground, climate change is expected to trigger acclamatory responses in vegetation that lead to the modification of eco-hydrological responses (23). In the context of the plant acclimation categorization presented by Drewry, et al. (23), these C4 crops do not show any significant structural (leaf area) or biochemical acclimation (photosynthetic down-regulation), with the primary response to elevated CO_2 being ecophysiological acclimation (decreased stomatal conductance), and associated decreases in canopy-scale transpiration. This conclusion is drawn based on Free Air CO_2 Enrichment (FACE) experiments which have demonstrated a lack of response of photosynthesis, biomass accumulation, and yield of maize under elevated CO_2 (24, 25). These experiments have also shown insensitivity of key photosynthetic enzymes of this C4 crop to elevated CO_2 (24), and have pointed to the alleviation of water stress as the primary impact of elevated CO_2 on maize productivity (26, 27), in agreement with previous hypotheses on the impact of elevated CO_2 on the func-

ENVIRONMENTAL SCIENCES

ECOLOGY

Author contributions: P.K. and D.T.D. designed research; P.V.V.L. and P.K. performed research; P.V.V.L. and D.T.D. analyzed data; and P.V.V.L., P.K., and D.T.D. wrote the paper.

The authors declare no conflict of interest.

This article is a PNAS Direct Submission.

[1]To whom correspondence should be addressed. E-mail: kumar1@illinois.edu.

This article contains supporting information online at www.pnas.org/lookup/suppl/doi:10.1073/pnas.1107177108/-/DCSupplemental.

tioning of C4 plants (28). Published results for the response of miscanthus and switchgrass to elevated CO_2 are not yet available. We have therefore adopted the maize response as prototypical of all three crops. Increases in the air temperature will likely increase *ET* losses, potentially offsetting the conservative impact of reduced stomatal conductance on transpiration. The combined impact of these counteracting effects is a complex function of the biophysical functioning of each crop type, resulting in potentially significant changes in canopy-integrated water and heat exchange with the atmosphere.

In this study, we explore potential hydrologic change associated with simultaneous land use conversion to bioenergy crops and projected climate change in the US Midwest. Specifically, we contrast the ecohydrological responses of maize, the main feedstock for current starch-based biofuel production, with miscanthus and switchgrass, through the application of a vertically resolved model of canopy biophysical processes. The simulations are performed by parameterizing a multilayer canopy model [MLCan; (22, 23)] to account for canopy structural and biophysical functional characteristics of miscanthus and switchgrass. The data and modeling framework is described in *Materials and Methods*. The MLCan model has been extensively validated for both ambient and elevated CO_2 conditions for maize (C4) and soybean (C3) (22, 23). A list of essential parameters and their values for maize, miscanthus, and switchgrass is presented in Table S1.

The study is performed in four stages. First, the model is run for the year 2005 when field observations of leaf photosynthetic CO_2 uptake (A_n), strongly correlated with water utilization (29, 30), are available for miscanthus and switchgrass, providing data for model validation. Second, we examine the alterations in the energy balance and canopy temperature that result from the land use conversion from maize to miscanthus and switchgrass under present climate in 2005. Third, as a single year of data does not capture the entire range of meteorological variability in the recent past, we use a stochastic weather generator (31) to provide an ensemble of forcing for the model (Fig. 1). This ensemble enables us to examine the range of crop responses to potential meteorological forcing. In the fourth stage, meteorological forcing ensembles are generated which capture climate variability associated with a number of climate change scenarios projected for the US Midwest for 2050 (32) (see Table 1). The model is forced using each of the climate scenarios to produce variability range corresponding to the hydrologic predictions associated with these future climate scenarios. We then estimate the water use of bioenergy crops and the impact on the hydrologic cycle which is characterized through the change in soil-water storage and specific surface runoff (runoff per unit area).

Results

Model Validation. Comparisons of modeled and observed (data obtained from ref. 33) photosynthetic leaf CO_2 uptake (A_n) for several days demonstrate the ability of the model to capture the ecophysiological functioning of both miscanthus and switchgrass throughout the growing season (Fig. 2). A_n for miscanthus is consistently higher than switchgrass throughout the growing season. The fluctuations of A_n for both crops are strong on some days (e.g., Jul 7th and Aug. 10th) and are an indicator of the tight link between A_n and environmental conditions. Variations in solar radiation due to cloudiness and the associated air temperature fluctuations are the primary drivers of variability in biochemical photosynthesis and stomatal conductance which in turn controls leaf temperature through the energy balance (22) (Fig. 1).

Within-Canopy Vertical Variation. The multilayer canopy-root-soil system model, MLCan, provides insights into the impact of the vertical distributions of leaf area and root biomass (22), presented in Fig. S1. The leaf area density (*LAD*) affects radiation attenuation through the canopy and canopy microclimate, while root

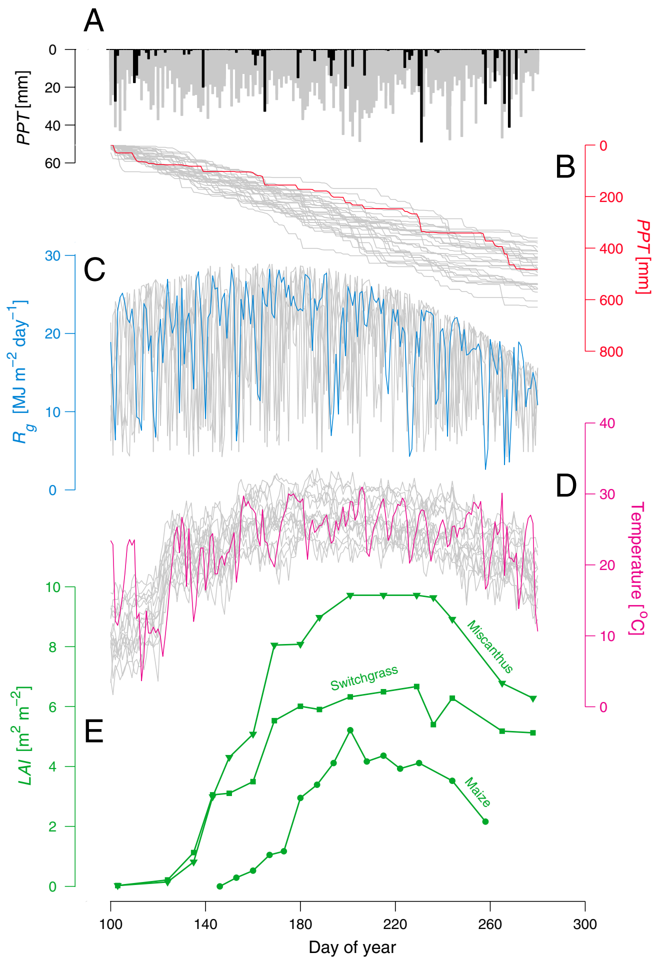

Fig. 1. Key meteorological forcing data observed in 2005 overlaid on an ensemble obtained using the stochastic weather generator. Meteorological data includes (*A*) Daily precipitation (*PPT*, black bars); (*B*) Cumulative precipitation (*PPT*, red line); (*C*) Daily global radiation (R_g, blue line); and (*D*) Mean day time air temperature (T_a, magenta line). Gray bars and lines in (*A, B, C, and D*) represent corresponding data obtained from stochastically generated weather ensemble of 30 independent years. All observed meteorological data in 2005 is obtained from Ameriflux tower at Bondville, Illinois (22). (*E*) *LAI* for the maize (green circles), miscanthus (green triangles), and switchgrass (green squares) canopies were obtained from published sources (11, 22). Miscanthus and switchgrass have a longer growing season as compared to maize, both at the beginning and end, which is reflected in the *LAI* plots.

biomass distribution dictates patterns of water uptake through the soil column. Fig. S2 presents the mean diurnal vertical patterns of A_n, latent heat (*LE*), sensible heat (*H*), total absorbed shortwave radiation (Q_{abs}), including photosynthetically active (*PAR*) and near-infrared (*NIR*) bands, and stomatal conductance for vapor (g_{sv}) through the canopy of each crop over the month of August, 2005. For each crop, the vertical distribution of A_n and

Table 1. Projected climate change scenarios during the summer for driving MLCan model predictions

Scenario	CO_2 [ppm]	Precipitation change [%]	Temperature increase [°C]
S-1	550	-	–
S-2	550	−15%	–
S-3	550	-	+1
S-4	550	-	+2
S-5	550	-	+3
S-6	550	−15%	+1
S-7	550	−15%	+2
S-8	550	−15%	+3

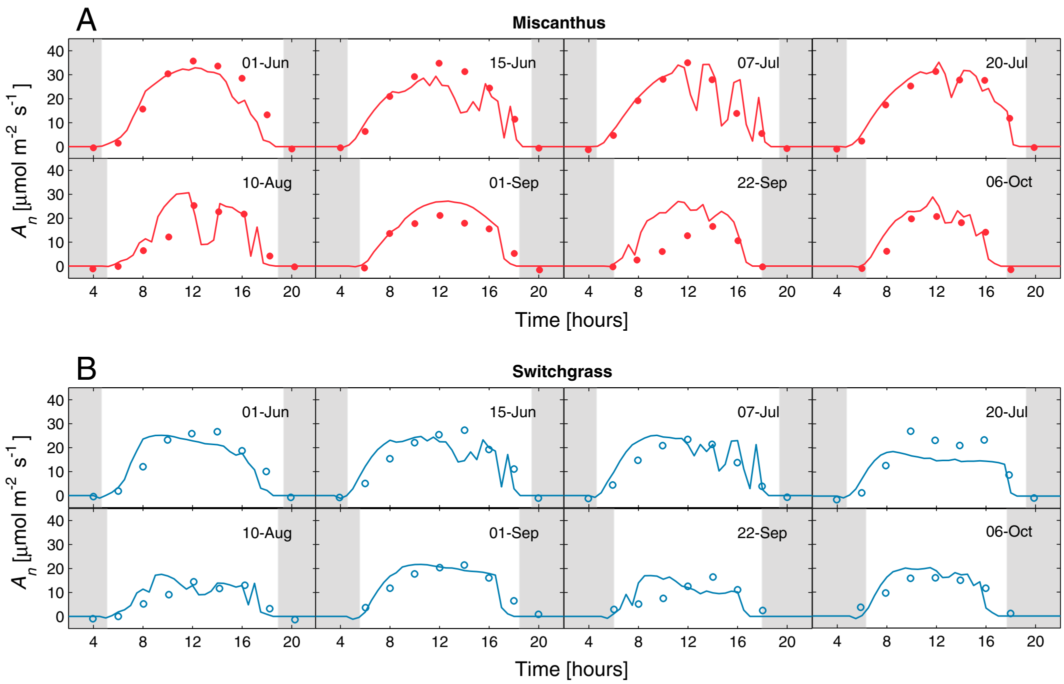

Fig. 2. Comparison of half-hourly net photosynthetic leaf CO_2 uptake (A_n) of upper canopy sunlit leaves for (*A*) miscanthus modeled by MLCan (red solid lines) and observed data (red circles) and (*B*) switchgrass modeled by MLCan (blue solid lines) and observed data (blue open circles). Observed data is obtained from Dohleman, et al. (33) on eight separate days during the growing season in 2005. Gray shading represents nighttime.

LE correspond closely to $Q_{\rm abs}$ as *PAR* is the primary driver of A_n, and $Q_{\rm abs}$ provides the majority of the energy partitioned into *LE* and *H* (22). In addition, g_{sv} is highest at the very top of the canopy where shortwave intensity is strongest. However, deeper distributions of positive *H* compared to A_n, *LE*, and $Q_{\rm abs}$ reflect the ability of *NIR* to penetrate deeper in the canopy (Fig. S2). Switchgrass has a smoother *LAD* profile than that of miscanthus (Fig. S1), which in combination with its lower canopy density (or *LAI*) (Fig. 1*E*), results in a more uniformly distributed radiation regime through the canopy, similar to that of maize (22). The much denser foliage of the miscanthus canopy, in combination with an upper canopy *LAD* maximum at $z/h = 0.75$ (Fig. S1), where *z* is the vertical coordinate and *h* is the canopy height, results in greater extraction of shortwave radiation in the upper third of the canopy, and a greater sink of CO_2 and source of energy relative to maize and switchgrass (Fig. S2). The denser miscanthus canopy more effectively shades the soil column below it, making the fraction of soil evaporation under miscanthus much smaller than for either switchgrass or maize (Table 2). The greater leaf area of miscanthus likewise increases interception of precipitation, and condensation, thereby increasing subsequent canopy evaporation (Table 2).

Impact of Crop Type on Energy Balance. The structural and ecophysiological differences in the three bioenergy crops examined here have implications for changes in surface temperature and albedo. Here we examine the relative effects of each canopy cover on mean surface temperature and albedo under present climate conditions (2005). The diurnal variations of mean canopy temperature under present conditions over one month (Aug. 2005) for miscanthus and switchgrass are slightly lower than those of maize (Fig. 3*A*). The largest differences between the mean canopy temperature of maize, and that of miscanthus (≈0.9 °C) and switchgrass (≈0.5 °C) occurs at approximately noon, when all three crops achieve their maximum canopy temperatures. This difference can be attributed to the increased dissipation of absorbed radiation by transpiration for miscanthus and switchgrass. Higher *LAI* for miscanthus results in a stronger decrease of mean canopy temperature than switchgrass, relative to maize.

Diurnal variation of temperature difference between top layers and mean canopy for three crops over the same time are also compared to evaluate their temperature variation through the canopy (Fig. 3*B*). Compared to other crops, maize shows a smaller

Table 2. Comparison of total evapotranspiration (*ET*) and its component contribution maize, miscanthus, and switchgrass under present climate condition in 2005

Crops	Maize	Miscanthus	Switchgrass
Total *ET* [mm]	380	588	498
Transpiration [mm]	302 (79.5%)	473 (80.5%)	402 (80.7%)
Canopy evaporation [mm]	36 (9.5%)	98 (16.6%)	66 (13.3%)
Soil evaporation [mm]	42 (11.0%)	17 (2.9%)	30 (6%)

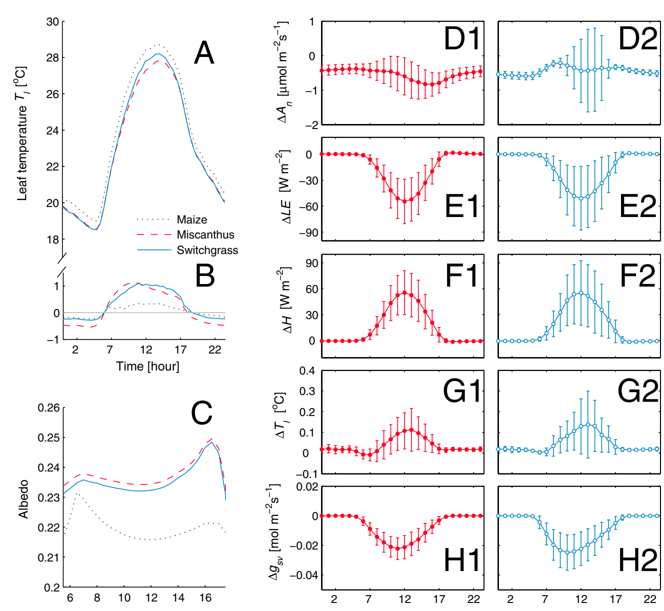

Fig. 3. Diurnal variation of mean canopy temperatures (*A*), temperature difference between the top layers and mean canopy (*B*), and albedo during the day (*C*) for maize (black dot line); miscanthus (red dash line); and switchgrass (blue solid line) in August 2005. Diurnally averaged change of net-canopy fluxes and variables obtained from the MLCan model with vertical bars representing ± one standard deviation over growing season of photosynthetic rate ΔA_n (*D*); Latent heat ΔLE (*E*); Sensible heat ΔH (*F*); Leaf temperature ΔT_l (*G*); Stomatal conductance for vapor Δg_{sv} (*H*) for miscanthus (in red—D1, E1, F1, G1, and H1); and switchgrass (in blue—D2, E2, F2, G2, and H2).

temperature fluctuation through the canopy due to lower *LAI*. Temperature differences between top layers and mean canopy for maize, miscanthus, and switchgrass ranged from −0.2 to 0.4 °C, −0.6 to 1.1 °C, and −0.3 to 1.1 °C, respectively.

However, diurnal variations of albedo during the daytime in August 2005 for the bioenergy crops are higher than maize (Fig. 3*C*). This higher albedo is because the lower *LAI* of maize allows more radiation to penetrate through the canopy to the soil which has a lower reflectivity than the leaves. Predicted mean values of albedo for miscanthus, switchgrass, and maize are 0.237, 0.235, and 0.220, respectively.

Vegetation Response to Elevated CO_2 and Increased Air Temperature. To understand how each crop responds to elevated CO_2, and in particular the impact of reduced stomatal conductance on canopy energy partitioning, the model was run for the 2005 "present climate" forcing with two different atmospheric CO_2 concentrations: one representing present conditions (370 ppm) and one representing projected concentrations for the year 2050 (550 ppm). Fig. 3 *D–H* show the diurnally averaged change of several net-canopy fluxes for miscanthus and switchgrass over four months of the growing season (June–Sept.), with each change (Δ) representing the difference between the 550 ppm and 370 ppm simulations. The diurnally averaged net-canopy fluxes over this same period under the 2005 climate forcing and atmospheric CO_2 concentration of 370 ppm is presented in Fig. S3 for comparison. The model's ability to incorporate ecophysiological acclimation of reduced stomatal conductance but no structural and biochemical acclimation (see Fig. 2 in ref. 22) for these C4 crops (24,27) to elevated CO_2 results in only small changes in A_n (<2%) for both miscanthus and switchgrass. However, reduced stomatal conductance causes a decrease in *LE* and a corresponding increase in *H* for both crops, with peak decreases in *LE* of 56 and 50 $W \cdot m^{-2}$, and an increase in *H* of 54 and 52 $W \cdot m^{-2}$ for miscanthus and switchgrass, respectively. The peak reduction in g_{sv} is −0.022 and −0.025 $mol\, m^{-2} \cdot s^{-1}$ for miscanthus and switchgrass, respectively. Fig. 3 *D–H* further shows that the diurnal variability of the net-canopy flux changes under elevated CO_2 for switchgrass are larger than those for miscanthus. These ecophysiological changes imply a reduction in water loss through *ET* under elevated CO_2. All three crops show a consistent decrease in total *ET* ranging from 40 to 70 mm over one growing season (Table 3). To evaluate the role of temperature on *ET* change, the model was run for the 2005 "present climate" with projected atmospheric CO_2 concentration (550 ppm), but for three scenarios of increased air temperature during the summer, ranging from 1 to 3 °C (32). In contrast to the results with a modification only to CO_2 concentration, as air temperature increases in a higher CO_2 environment, the advantage of reduced water use is lost due to the increase of total *ET* (Table 3). The reason is that higher air temperature not only increases water evaporation from the soil and canopy but also modulates transpiration rate through its effect on vapor pressure (34).

Table 3. Comparisons of total evapotranspiration (*ET*) alterations [mm] under climate change between maize, miscanthus, and switchgrass

	Total *ET* change [mm] under elevated CO_2			
Crops	$T_a + 0°C$	$T_a + 1°C$	$T_a + 2°C$	$T_a + 3°C$
Maize	−40	−10	15	40
Miscanthus	−70	−17	19	53
Switchgrass	−47	5	20	49

ET under elevated CO_2 and at different levels of increased air temperature (T_a) are compared with *ET* under present condition for each crop*. Elevated CO_2 is set equal to 550 ppm

*$\Delta ET^{crop} = ET^{crop}_{future} - ET^{crop}_{present}$

Impact on Hydrology. Changes in weekly mean water balance components for the three crops are compared under the same weather condition of the year 2005 (Fig. S4). The water use of miscanthus is the highest while that of maize is the lowest, further reflecting the role of *ET* as a key determinant of the water balance. Transpiration is the largest component of the water balance, accounting for more than 80% of total *ET* (see Table 2). A conversion from maize to miscanthus or switchgrass will lead to a reduction in soil-water storage and a consequent reduction in specific runoff. Under present climate in 2005, the total decreases in soil-water storage are 115 and 63 mm for miscanthus and switchgrass, respectively, relative to maize. The corresponding decrease in specific surface runoff are 24 and 6 mm, respectively.

To capture the uncertainty associated with these estimates, the model was run using an ensemble of thirty years of weather forcing obtained using a stochastic weather generator (31) (described in *Materials and Methods*). To understand the possible range of variation for each projected climate scenario the weather ensemble was modified to represent the conditions summarized in Table 1. Fig. 4 shows the box plots of total *ET*, soil-water storage change, and total specific surface runoff if maize is replaced by miscanthus or switchgrass. Under projected climate change scenarios our simulations demonstrate that there will be a decrease in both soil-water storage and specific surface runoff.

In the first scenario (elevated CO_2) soil-water storage and specific surface runoff decrease the least, as increased transpiration loss due to denser canopies and longer growing seasons is somewhat offset by reductions in stomatal conductance associated with ecophysiological acclimation. The mean soil-water storage decreases approximately 110 mm for miscanthus and 40 mm for switchgrass. For mean total specific surface runoff, the decreases are 25 and 3 mm, respectively.

In the second scenario, as precipitation is decreased 15% in the summer (32), water storage and surface runoff are further decreased, highlighting the role of reduced water availability.

In scenarios 3–5, air temperature is increased at three levels without any change in precipitation. We found that the decrease of total water storage and surface runoff is directly dependent on the increase of air temperature. Mean soil-water storage decreases ranged from 160 to 240 mm and 70 to 120 mm for miscanthus and switchgrass, respectively, for temperature increases ranging from 1 to 3 °C.

For scenarios 6–8, air temperature is increased at three levels along with the 15% reduction in precipitation. Water storage decreases are slightly greater than those in scenarios 3–5 due to the further reduction in water input.

The fractions of soil-water storage and specific surface runoff change during the overlapping and longer growing seasons (with respect to maize) of both bioenergy crops are also different. For miscanthus, 87% of soil-water storage change occurred during the overlapping period of the growing season, and 13% due to water utilization during the longer growing season. For switchgrass, these estimates are 83% and 17%, respectively. However, both crops showed a 92% decrease of specific surface runoff during the overlapping period of the growing season, and 8% decrease in the longer growing season.

Discussion

National policies and economic viability are likely to foster a shift in agricultural practices from maize to bioenergy crops such as miscanthus and switchgrass (35). The differences of miscanthus and switchgrass from maize in the density (*LAI*) and architecture (*LAD*) of above-ground foliage results in increased transpiration. The difference in structure also facilitates larger interception of rainfall and condensation leading to increased direct evaporation from the foliage. Attenuation of radiation through the denser canopy reduces the radiation reaching the soil thereby increasing the albedo as more light is reflected from the more reflective

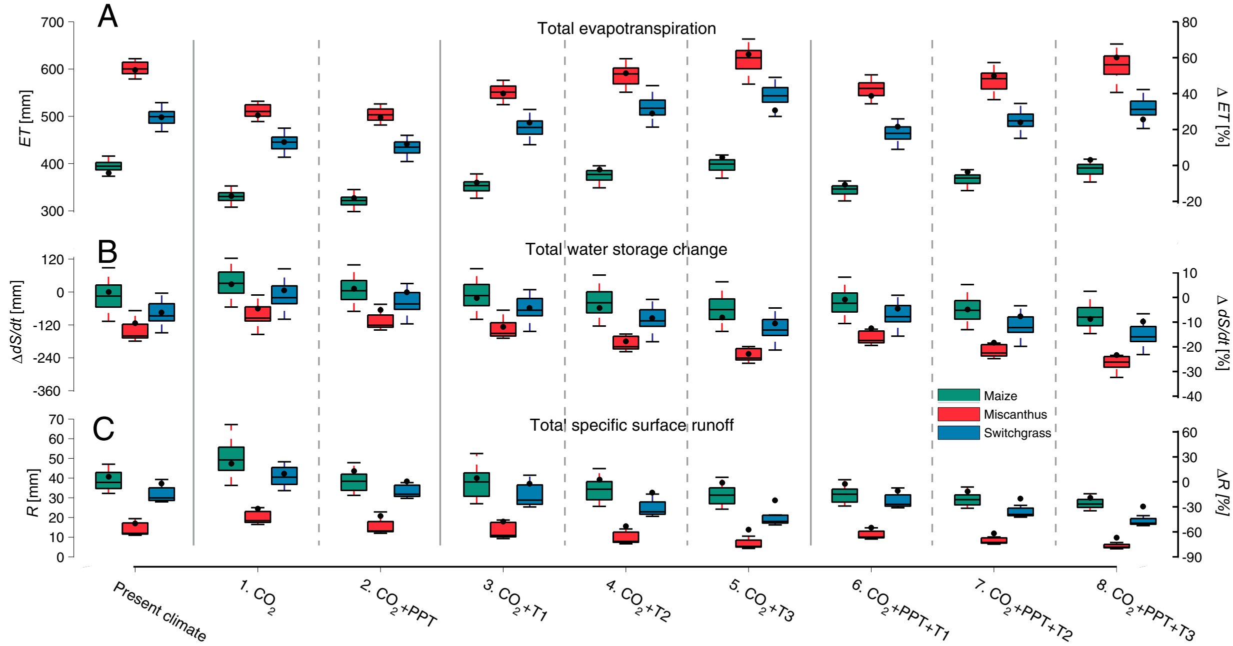

Fig. 4. Ensemble of total evapotranspiration (*A*), total soil-water storage change (*B*), and total specific surface runoff (*C*) for maize (green), miscanthus (red), and switchgrass (blue) under present climate and eight combinations of climate change scenarios involving expected CO_2 concentration, higher air temperature, and altered precipitation magnitudes (32). The right axes represent percentage change with the median value of maize in the present climate as baseline. Forcing data in each scenario is obtained from stochastically generated weather ensemble of 30 independent years. Black dots represent the MLCan predictions corresponding to 2005 or projections based on 2005 observations. Vertical solid and dash lines separate different scenarios.

foliage and reducing soil evaporation. All these factors impact both the energy and water balance. Elevated atmospheric CO_2 concentrations lead to an ecophysiological reduction in stomatal conductance of the C4 plants which results in a suppression of transpiration and a corresponding increase in soil-water storage and specific runoff. However, this conservation is not sufficient to offset the reductions induced by the land use change from maize to miscanthus and switchgrass. When expected increase in air temperature and reductions in rainfall are further included, the conservative advantage of elevated CO_2 is lost resulting in large reductions of both soil-water storage and specific runoff. Miscanthus, by virtue of its significantly larger *LAI*, has the larger impact among the two bioenergy crops. Additionally, the longer growing season adds to the net reduction in storage and runoff but this accounts for roughly 15% of the change while the remainder is due to the structural differences in the vegetation foliage. As illustrated in Fig. 4, the increase in evapotranspiration, and reductions in soil-water storage and specific surface runoff are quite large, but these per unit area estimates need to be factored in with the fraction of land use conversion to get estimates of watershed scale impacts. For extensive areal alterations, the impact of bioenergy crops on the runoff and the local environment from increased atmospheric humidity due to transpiration can be quite significant. These issues should be weighed together with other environmental and energy and economic benefits.

Materials and Methods

Multilayer Canopy Model. Simulations are performed using the vertically resolved canopy-root-soil model MLCan (22, 23). MLCan incorporates explicit coupling between leaf-level ecophysiological processes (photosynthesis and stomatal conductance), physical processes (energy balance and boundary layer conductance), and below-ground water status which incorporates a hydraulic redistribution model (36). MLCan resolves the short- and long-wave radiation regimes throughout the vertical canopy space. Radiation attenuation is in large part determined by the vertical distribution of foliage. MLCan provides predictions of photosynthetic CO_2 assimilation and respiratory losses, as well as latent and sensible heat fluxes for each canopy layer, through considerations of energy balance for both sunlit and shaded leaf fractions. Water storage on foliage, as a function of dew or rainfall interception, is likewise considered. The model has been validated for both C3 and C4 vegetation (22) and evaluated for its ability to capture acclimatory responses of vegetation to elevated CO_2 (23).

The model is first run using meteorological forcing and observed *LAI* data for 2005 reported in Heaton, et al. (11) (Fig. 1). For the present conditions, atmospheric concentration of CO_2 is set equal to 370 ppm (37). This simulation is used for model validation using observed A_n of upper canopy sunlit leaves during the growing season (33). Second, we incorporate stochastically generated weather ensemble data consisting of 30 independent years with climate change projections in the Midwest (32) for driving the MLCan model to predict water use by energy crops. Under climate change, atmospheric concentration of CO_2 is set equal to 550 ppm while precipitation patterns in the Midwest are expected to decrease 15% in the summer and increase 10% in the winter at the middle of the 21st century (32). In addition, expected average increase in temperature ranges from 1 to 3 °C in the summer and from 0.3 to 1 °C in the winter. To evaluate the role of temperature increase, we further conducted an air temperature sensitivity analysis to the water uses by increasing air temperature at three levels in both summer and winter seasons. However, vegetation growth period mostly spans the summer season. We also conducted predictions for both change and no change in precipitation pattern to assess the role of water availability on the predictions (Table 1).

Meteorological Data. Half-hourly meteorological data are obtained from AmeriFlux tower (http://public.ornl.gov/ameriflux) located in Bondville, Illinois (40.01°N, 88.29°E). Data in the growing season 2005 is used for MLCan model validation. Observed data from 1997–2006 at this tower, and cloud cover data at the nearby University of Illinois Willard Airport obtained from National Climatic Data Center (http://www.ncdc.noaa.gov/oa/ncdc.html) are used for parameterizing the stochastic weather generator.

Ecophysiological Data. Ecophysiological data is also collected in central Illinois. *LAI* data for miscanthus and switchgrass is obtained from a published source (11) with approximately biweekly measurements from emergence to senescence at three locations very close to the Bondville tower during 2005. Each location has four plots of 10m × 10m for both miscanthus and switchgrass. Observations for A_n of upper canopy sunlit leaves are obtained from another published source (33). These observations were made at 2 h intervals from predawn to postdusk on eight separate days across the growing season in 2005 in the same plots as studied by Heaton, et al. (11).

Canopy, Soil, and Root System. Canopy structure is described by *LAD* profiles and the total *LAI*. Vertical distributions of leaf area through the canopy for miscanthus (38) and for switchgrass (39) are averaged and normalized by dividing the canopy *LAI* at the time of measurement (Fig. S1*A*). Distributions of root systems through the soil column for miscanthus and switchgrass are obtained from the study by Monti and Zatta (40) (Fig. S1*B*). Canopy and root structures of maize are obtained from our previous work (22). Initial condition of soil moisture is set equal to 30% (22).

Weather Generator. Stochastic weather generator developed by Ivanov, et al. (31) is used for developing a forcing ensemble. The weather generator provides Monte Carlo simulation for hourly data which are then linearly interpolated to obtain half-hour values corresponding to the model time step. Parameters for the generator are obtained from 10-year (1997–2006) observation time series at the flux tower. The stochastic generator should be expected to capture the range of variability observed during this time period (see Fig. 1). An ensemble of 30 independent years of weather simulation is used for each case in the study.

Water Balance. Change in soil-water storage is important for evaluating the impact of different land covers on the hydrologic cycle. It is given as:

$$\frac{\mathrm{dS}}{\mathrm{dt}} = P + C - T_R - E - S_E - S_P - R, \qquad [1]$$

where P, C, T_R, E, S_E, S_P, and R represent precipitation, condensation, transpiration, evaporation, soil evaporation, seepage, and specific surface runoff. All variables are in the dimensions of $[L/T]$.

Calculation of Albedo. Albedo for each crop is estimated based on the ratio of total outgoing and incoming shortwave radiation during the daytime.

$$\alpha = \frac{\int_{\mathrm{SW}^{\downarrow}>40(\mathrm{W\cdot m^{-2}})} \mathrm{SW}^{\uparrow}\mathrm{dt}}{\int_{\mathrm{SW}^{\downarrow}>40(\mathrm{W\cdot m^{-2}})} \mathrm{SW}^{\downarrow}\mathrm{dt}} \qquad [2]$$

α: albedo [dimensionless];
$\mathrm{SW}^{\downarrow}$: downward or incoming shortwave radiation ($\mathrm{W\cdot m^{-2}}$);
$\mathrm{SW}^{\uparrow}$: upward or outgoing shortwave radiation ($\mathrm{W\cdot m^{-2}}$).

Sensitivity to Seasonal Variation in Photosynthetic Capacity. Considerations for structural, biochemical, and ecophysiological acclimation responses under elevated CO_2 have been made following the methodology of Drewry, et al. (23). For C4 crops, the simulations are performed for a constant value for $V_{\max}$ for the growing season (Table S1). We have examined the impact of seasonal variations in $V_{\max}$ for maize following observations presented in a study by Markelz, et al. (41). We assumed that the beginning and end of the growing season values are the same and correspond to the low value for the season with a high value in the early half of the season (see Fig. S5). Seasonality of $V_{\max}$ has little impact on the canopy fluxes (See Fig. S6) and results in a small change in total ET (1.8%) and specific surface runoff (1.7%) in comparison to the constant $V_{\max}$ case (Table 2). Similarly, simulations performed with a seasonally high but constant value of $V_{\max}$ result in only small changes in the fluxes for maize (See Fig. S6, Table S2). Data on seasonal variation of $V_{\max}$ for miscanthus and switchgrass is not available, but given the lack of any significant response in maize, it is deemed that the results with constant value (Table S1) capture the tendencies well.

ACKNOWLEDGMENTS. This work was supported by Vietnam Education Foundation (VEF) and National Science Foundation (NSF) Grant ATM 06-28687. D.T.D. was also supported by the National Science Foundation's International Research Fellowship Program (IRFP), award OISE-0900556.

1. Ragauskas AJ, et al. (2006) The path forward for biofuels and biomaterials. *Science* 311:484–489.
2. Wall JD, Harwood CS, Demain AL (2008) *Bioenergy* (ASM Press, Washington, DC).
3. Kladivko EJ (2001) Tillage systems and soil ecology. *Soil Till Res* 61:61–76.
4. Donner SD (2007) Surf or turf: a shift from feed to food cultivation could reduce nutrient flux to the Gulf of Mexico. *Global Environ Chang* 17:105–113.
5. Schnoor JL, et al. (2008) *Water implications of biofuels production in the United States* (National Academies Press, Washington, DC).
6. Costello C, Griffin WM, Landis AE, Matthews HS (2009) Impact of biofuel crop production on the formation of hypoxia in the Gulf of Mexico. *Environ Sci Technol* 43:7985–7991.
7. Tilman D, Hill J, Lehman C (2006) Carbon-negative biofuels from low-input high-diversity grassland biomass. *Science* 314:1598–1600.
8. Cai X, Zhang X, Wang D (2011) Land availability for biofuel production. *Environ Sci Technol* 45:334–339.
9. Schmer M, Vogel K, Mitchell R, Perrin R (2008) Net energy of cellulosic ethanol from switchgrass. *Proc Natl Acad Sci USA* 105:464–469.
10. Hess JR, Thomas DF, Hoskinson R, Thompson D (2003) *Roadmap for agriculture biomass feedstock supply in the United States* (US Department of Energy, Washington, DC), DOE/NE-ID-11129, p 98.
11. Heaton EA, Dohleman FG, Long SP (2008) Meeting US biofuel goals with less land: the potential of miscanthus. *Glob Change Biol* 14:2000–2014.
12. Heaton EA, Voigt T, Long SP (2004) A quantitative review comparing the yields of two candidate C4 perennial biomass crops in relation to nitrogen, temperature and water. *Biomass Bioenerg* 27:21–30.
13. Dondini M, Groenigen KJV, Galdo ID, Jones MB (2009) Carbon sequestration under miscanthus: a study of 13 c distribution in soil aggregates. *Global Change Biology Bioenergy* 1:321–330.
14. Liebig MA, Schmer MR, Vogel KP, Mitchell RB (2008) Soil carbon storage by switchgrass grown for bioenergy. *Bioenergy Resources* 1:215–222.
15. Clifton-Brown JC, Breuer J, Jones MB (2007) Carbon mitigation by the energy crop, miscanthus. *Glob Change Biol* 13:2296–2307.
16. Ma Z, Wood CW, Bransby DI (2000) Soil management impacts on soil carbon sequestration by switchgrass. *Biomass Bioenerg* 18:469–477.
17. Hickman GC, Vanloocke A, Dohleman FG, Bernacchi CJ (2010) A comparison of canopy evapotranspiration for maize and two perennial grasses identified as potential bioenergy crops. *Global Change Biology Bioenergy* 2:157–168.
18. McIsaac GF, David MB, Mitchell CA (2010) Miscanthus and switchgrass production in central illinois: impacts on hydrology and inorganic nitrogen leaching. *J Environ Qual* 39:1790–1799.
19. Vanloocke A, Bernacchi CJ, Twine TE (2010) The impacts of miscanthus × giganteus production onthe Midwest US hydrologic cycle. *Global Change Biology Bioenergy* 2:180–191.
20. Pieruschka R, Huber G, Berry JA (2010) Control of transpiration by radiation. *Proc Natl Acad Sci USA* 107:13372–13377.
21. Sauer TJ, Singer JW, Prueger JH, DeSutter TM, Hatfield JL (2007) Radiation balance and evaporation partitioning in a narrow-row soybean canopy. *Agricultural and Forest Meteorology* 145:206–214.
22. Drewry D, et al. (2010a) Ecohydrological responses of dense canopies to environmental variability: 1. Interplay between vertical structure and photosynthetic pathway. *J. Geophys Res* 115:G04022, doi:10.1029/2010JG001340.
23. Drewry D, et al. (2010b) Ecohydrological responses of dense canopies to environmental variability: 2. Role of acclimation under elevated CO_2. *J Geophys Res* 115: G04023, doi:10.1029/2010JG001341.
24. Leakey ADB, et al. (2006) Photosynthesis, productivity, and yield of maize are not affected by open-air elevation of CO_2 concentration in the absence of drought. *Plant Physiol* 140:779–790.
25. Long SP, Ainsworth EA, Rogers A, Ort DR (2004) Rising atmospheric carbon dioxide: plants FACE the Future*. *Annu Rev Plant Biol* 55:591–628.
26. Leakey ADB, et al. (2009) Elevated CO_2 effects on plant carbon, nitrogen, and water relations: six important lessons from FACE. *J Exp Bot* 60:2859–2876.
27. Leakey ADB, Bernacchi CJ, Dohleman FG, Ort DR, Long SP (2004) Will photosynthesis of maize (*Zea mays*) in the US Corn Belt increase in future $[CO_2]$ rich atmosphere? An analysis of diurnal courses of CO_2 uptake under free-air concentration enrichment (FACE). *Glob Change Biol* 10:951–962.
28. Ghannoum O, von Caemmerer S, Ziska LH, Conroy JP (2000) The growth response of C-4 plants to rising atmospheric CO_2 partial pressure: a reassessment. *Plant Cell Environ* 23:931–942.
29. Knapp AK, Hamerlynck EP, Owensby CE (1993) Photosynthetic and water relations responses to elevated CO_2 in the C4 grass andropogon gerardii. *Int J Plant Sci* 154:459–466.
30. Nobel PST (1980) Water vapor conductance and CO_2 uptake for leaves of a C4 desert grass, hilaria rigida. *Ecology* 6:252–258.
31. Ivanov VY, Bras RL, Curtis DC (2007) A weather generator for hydrological, ecological, and agricultural applications. *Water Resour Res* 43:W10406.
32. Wuebbles DJ, Hayhoe K (2004) Climate change projections for the United States midwest. *Mitigation and Adaptation Strategies for Global Change* 9:335–363.
33. Dohleman FG, Heaton EA, Leakey ADB, Long SP (2009) Does greater leaf-level photosynthesis explain the larger solar energy conversion efficiency of miscanthus relative to switchgrass? *Plant Cell Environ* 32:1525–1537.
34. Hopkins WG, Huner NPA (2009) *Introduction to Plant Physiology* (John Wiley & Son, Inc, New Jersey).
35. Chen X, Huang H, Khanna M, Önal H (2011) *Meeting the Mandate for Biofuels: Implications for Land Use, Food and Fuel Prices* (Natl. Bureau Econ. Res, Cambridge, MA), National Bureau of Economic Research Working Paper No. 16697.
36. Amenu GG, Kumar P (2008) A model for hydraulic redistribution incorporating coupled soil-root moisture transport. *Hydrol Earth Syst Sc* 12:55–74.
37. Houghton JT, et al. (2001) *Climate Change 2001: The Scientific Basis* (Cambridge University Press, Cambridge, United Kingdom).
38. Kromdijk J, et al. (2008) Bundle sheath leakiness and light limitation during C4 leaf and canopy CO_2 uptake. *Plant Physiol* 148:2144–2155.
39. Madakadze IC, et al. (1998) Leaf area development, light interception, and yield among switchgrass populations in a short-season area. *Crop Sci* 38:827–834.
40. Monti A, Zatta A (2009) Root distribution and soil moisture retrieval in perennial and annual energy crops in northern Italy. *Agr Ecosyst Environ* 132:252–259.
41. Markelz RJC, Strellner RS, Leakey ADB (2008) Impairment of C4 photosynthesis by drought is exacerbated by limiting nitrogen and ameliorated by elevated $[CO_2]$ in maize. *J Exp Bot* 62:3235–3246.

Supporting Information

Le et al. 10.1073/pnas.1107177108

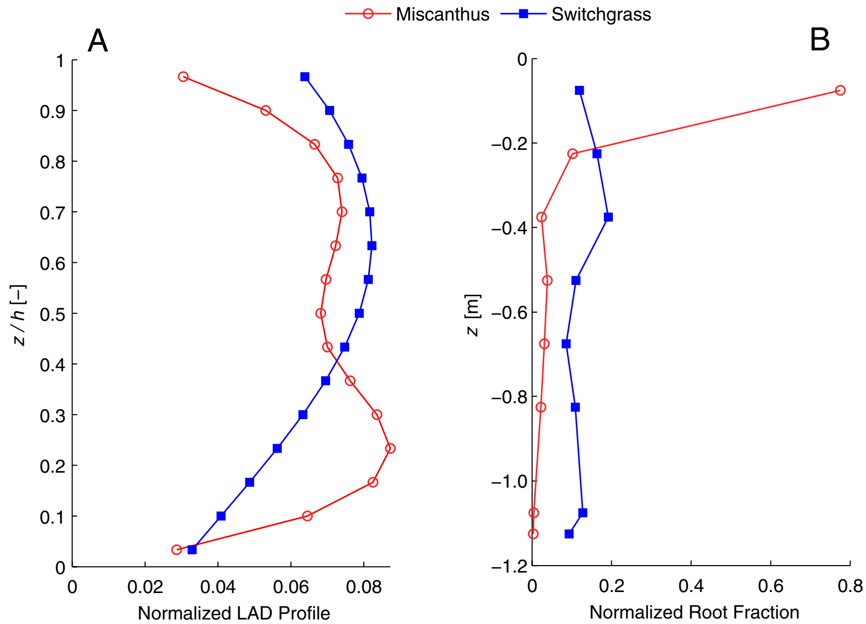

Fig. S1. Normalized canopy leaf area density profiles (*A*) and normalized root fraction in each soil layer (*B*) for miscanthus (red circles) and switchgrass (blue squares). The vertical axis in (*A*) is normalized by the height of the canopy (3.5 m for miscanthus, 2.0 m for switchgrass) to facilitate comparison between the two crops (based on data obtained from refs. 1, 2, 3).

1 Monti A, Zatta A (2009) Root distribution and soil moisture retrieval in perennial and annual energy crops in northern Italy. *Agr Ecosyst Environ* 132:252–259.
2 Kromdijk J, et al. (2008) Bundle sheath leakiness and light limitation during c4 leaf and canopy co2 uptake. *Plant Physiol* 148:2144–2155.
3 Madakadze IC, et al. (1998) Leaf area development, light interception, and yield among switchgrass populations in a short-season area. *Crop Sci*. 38:827–834.

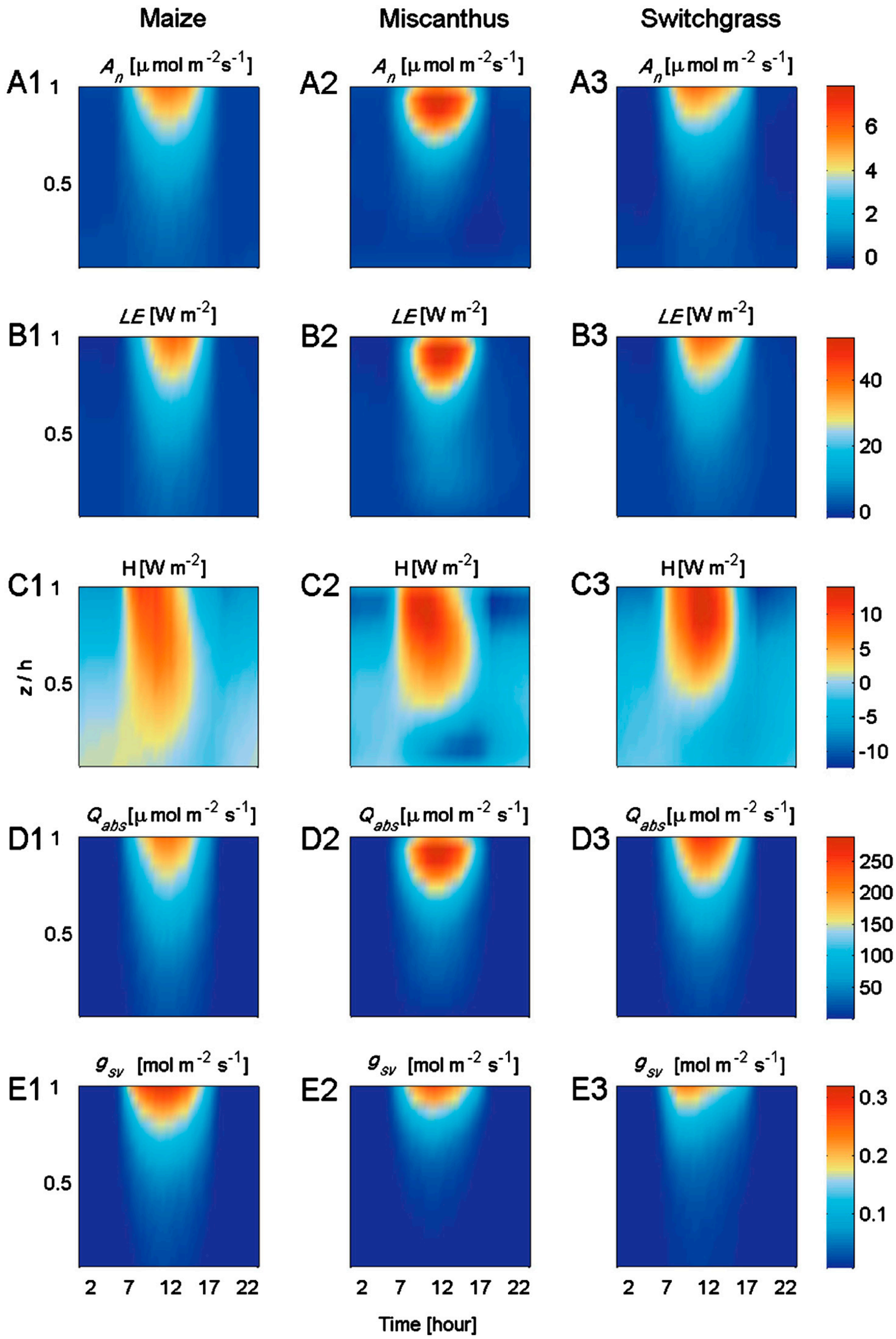

Fig. S2. Diurnally averaged profiles obtained from MLCan model simulation under present climate condition in August 2005 for photosynthetic rate A_n; latent heat LE; sensible heat H; total absorbed shortwave radiation included photosynthetically active and near-infrared bands Q_{abs}; and stomatal conductance for vapor g_{sv} for maize (left column—A1, B1, C1, D1, and E1), miscanthus (center column—A2, B2, C2, D2, and E2), and switchgrass (right column—A3, B3, C3, D3, and E3).

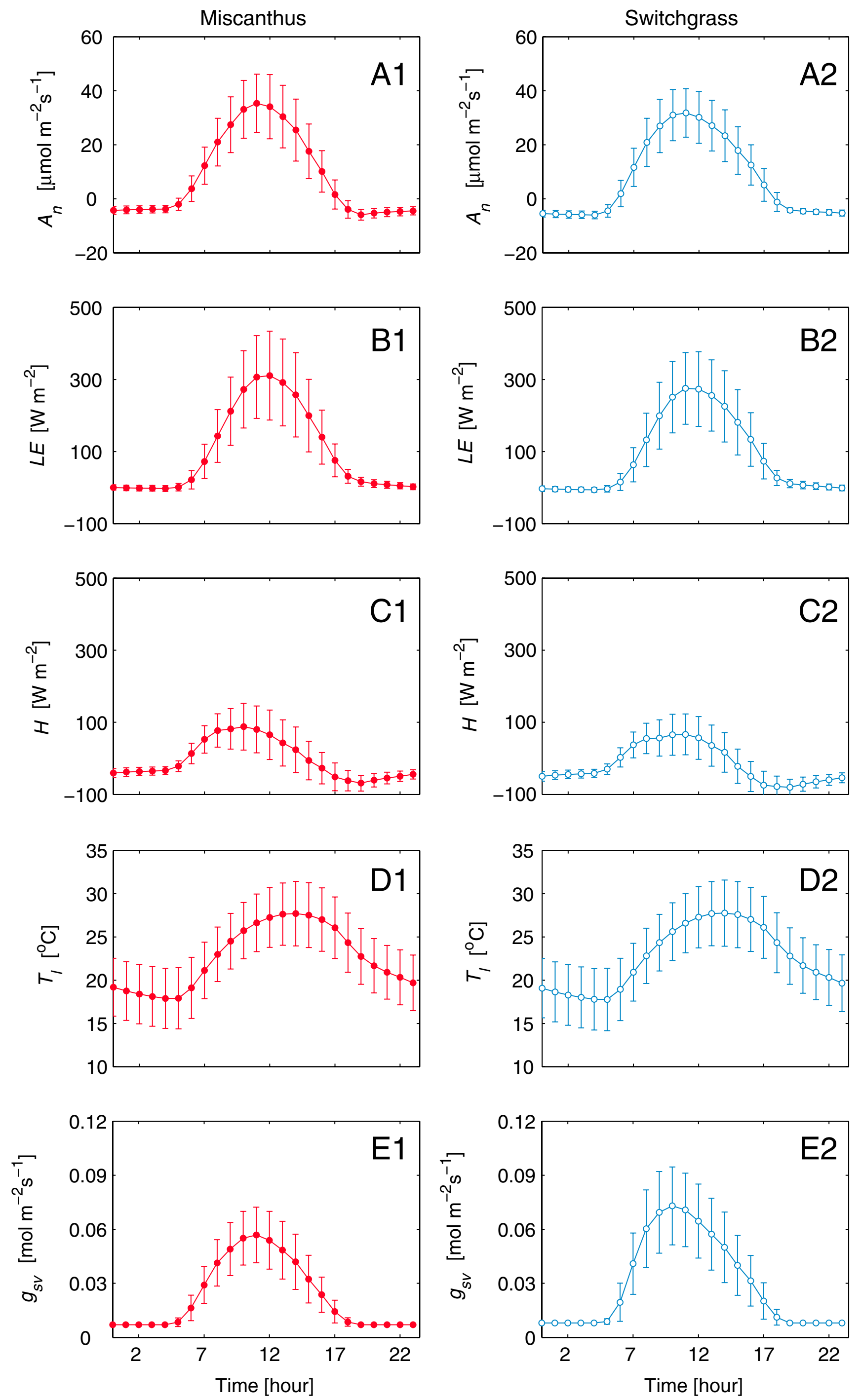

Fig. S3. Diurnally averaged net-canopy fluxes and variables obtained from the MLCan model under present climate condition in 2005 with vertical bars representing ± one standard deviation over one growing season of (*A*) Photosynthetic rate A_n; (*B*) Latent heat *LE*; (*C*) Sensible heat *H*; (*D*) Leaf temperature T_l; and (*E*) Stomatal conductance for vapor g_{sv} for miscanthus (in red—A1, B1, C1, D1, and E1) and switchgrass (in blue—A2, B2, C2, D2, and E2).

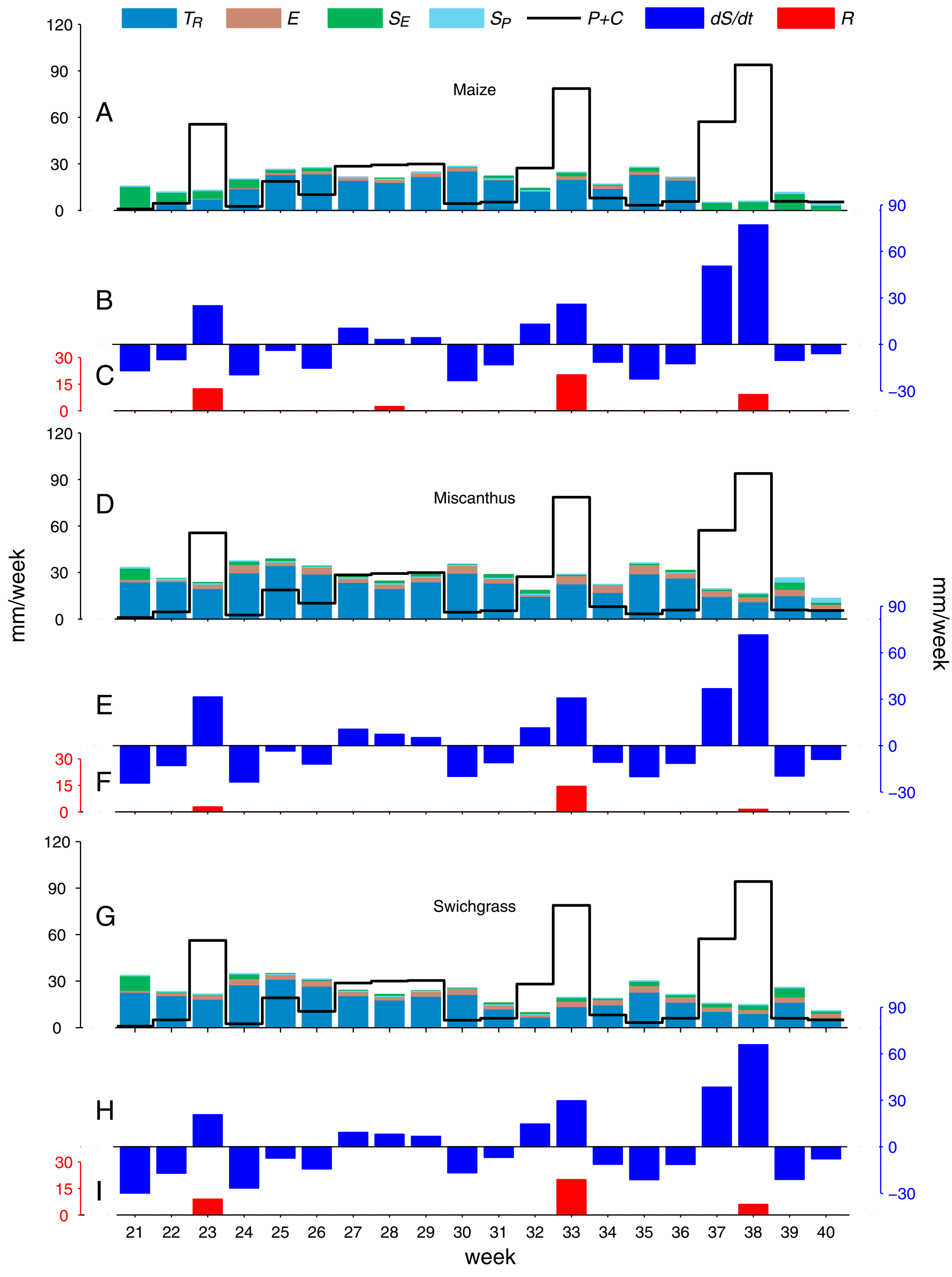

Fig. S4. Weekly mean water balance, soil-water storage change, and total specific surface runoff obtained using MLCan for three crops during several weeks in the 2005 growing season under present CO_2 conditions (370 ppm). (*A*, *D*, *G*) Weekly mean water balance; (*B*, *E*, *H*) weekly change of soil water storage dS/dt; and (*C*, *F*, *I*) total specific surface runoff for maize, miscanthus, and switchgrass, respectively. Black solid lines in (*A*, *D*, *G*) represents the total weekly precipitation *P* and condensation *C* on foliage (incoming water). Color boxes in (*A*, *D*, *G*) represent outgoing water components include: Transpiration T_R (dark blue); Evaporation *E* (brown); Soil Evaporation S_E (green); Seepage S_P (cyan). Note that: the first two and last four weeks are outside of the maize growing season.

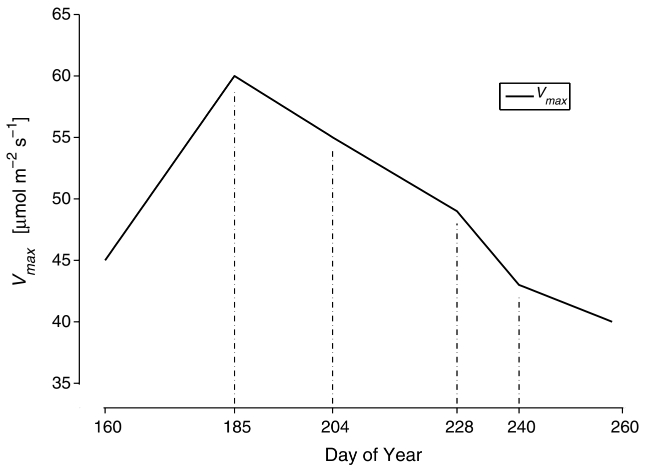

Fig. S5. To understand the impact of seasonality of leaf photosynthetic capacity on the results presented earlier, $V_{\max}$ for maize was varied as shown here. The values of $V_{\max}$ from day 185 to the end of the growing season was obtained and interpolated linearly from the study by Markelz, et al. (1). We also assumed a linear increase of $V_{\max}$ at the beginning of the season until it reached the maximum value at day 185 (2, 3).

1 Markelz RJC, Strellner RS, Leakey ADB (2008) Impairment of C4 photosynthesis by drought is exacerbated by limiting nitrogen and ameliorated by elevated [CO_2] in maize. *J Exp Bot* 62:3235–3246.

2 Wilson KB, Baldocchi DD, Hanson PJ (2000) Spatial and seasonal variability of photosynthetic parameters and their relationship to leaf nitrogen in a deciduous forest. *Tree Physiol* 20:565–578.

3 Xu L, Baldocchi DD (2003) Seasonal trends in photosynthetic parameters and stomatal conductance of blue oak (Quercus douglasii) under prolonged summer drought and high temperature. *Tree Physiol* 23:865–877.

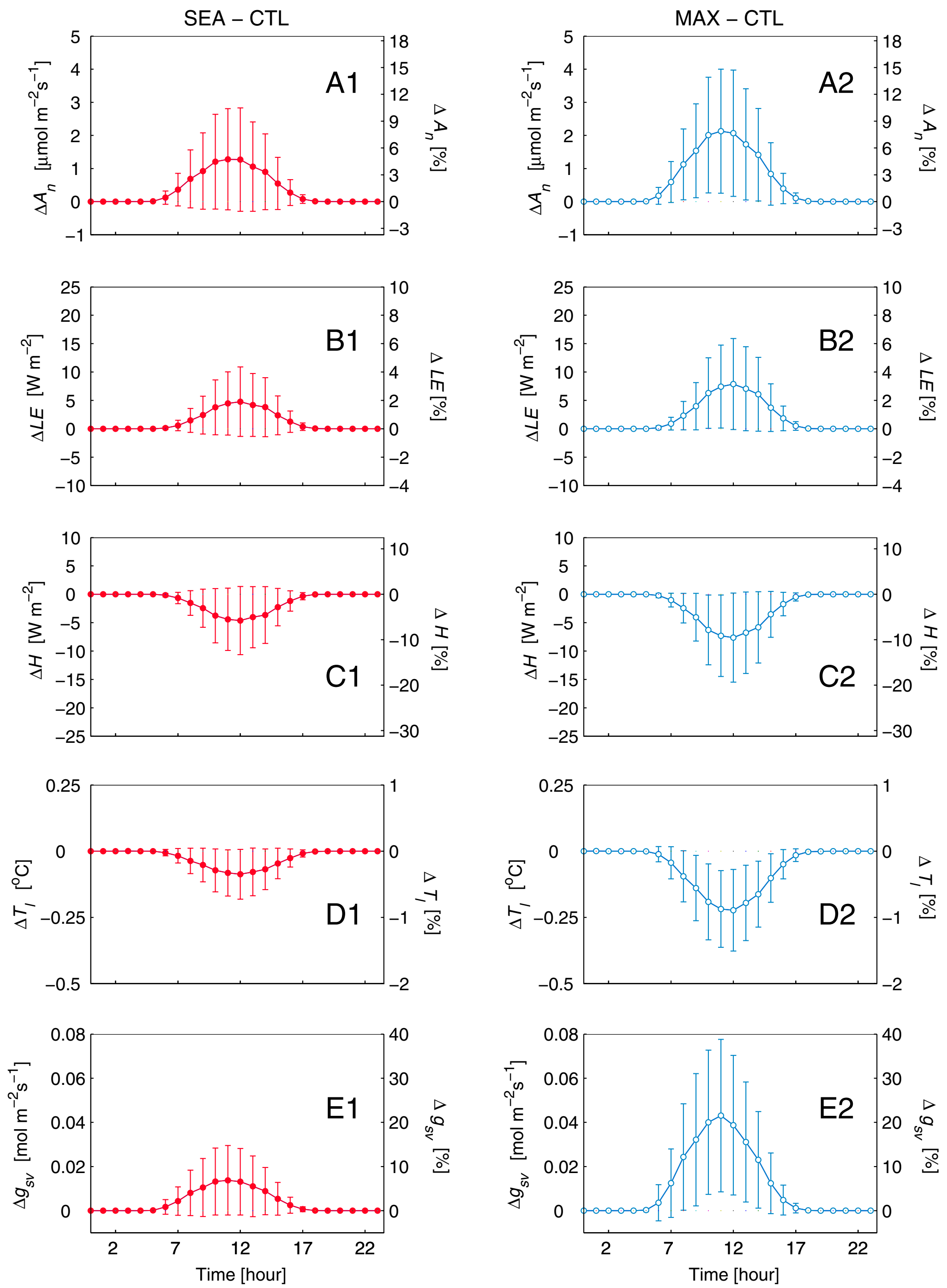

Fig. S6. Diurnally averaged change of net-canopy fluxes and variables obtained for maize during 2005 using the MLCan model with vertical bars representing ± one standard deviation over one growing season of (*A*) Photosynthetic rate A_n; (*B*) Latent heat *LE*; (*C*) Sensible heat *H*; (*D*) Leaf temperature T_l; and (*E*) Stomatal conductance for vapor g_{sv}. SEA represents the case with seasonal variation of V_{max} as shown in Fig. S5, CTL represents the control case presented earlier and MAX represents the situation when V_{max} is set to a constant but at seasonally high value of 60 μmol m^{-2} s^{-1}. The differences between SEA and CTL cases are presented in red (A1, B1, C1, D1, and E1) while differences between MAX and CTL are presented in blue (A2, B2, C2, D2, and E2). The right axes represent percentage change with respect to the maximum diurnally averaged value in the corresponding CTL simulation for maize.

Table S1. Value of model parameters for maize, miscanthus, and switchgrass used in the multilayer canopy-root-soil model (MLCan)

Description	Symbols	Unit	Maize*	Miscanthus	Switchgrass
Canopy height	h_{can}	m	2.5	3.5 (1)	2.0 (2)
Leaf width	d_o	m	0.08	0.03	0.01
Decay coefficient for leaf nitrogen content	k_n	-	0.5	0.15	0.4
Leaf emissivity	ϵ_v	-	0.94	0.95 (3)	0.95 (3)
Leaf absorptivity to photosynthetic active radiation (PAR)	$\alpha_{L\text{-PAR}}$	-	0.80	0.84 (1, 4)	0.8 (5)
Leaf absorptivity to near-infrared (NIR)	$\alpha_{L\text{-NIR}}$	-	0.23	0.2 (5)	0.2 (5)
Diffuse extinction coefficient	K_d	-	0.55	0.68 (6)	0.67 (2)
Leaf angle distribution parameter	x	-	1.64	1.64	1.64
Intrisic quantum yield C_4 photosynthesis	α	mol mol^{-1}	0.035	0.035	0.034
Initial slope of C4 photosynthetic CO_2 response	k_4	mol m^{-2} s^{-1}	0.7	0.7	0.7
Reference value fo leaf respiration	R_d	μ mol m^{-2} s^{-1}	0.8	0.8	0.6
Reference value for substrate saturated Rubisco capacity	V_{max}	μ mol m^{-2} s^{-1}	40	66	48
Temperature sensitivity of temperature-dependent C_4 parameters	$Q_{10,4}$	-	2.0	2.5	0.5
Stomatal slope parameter in Ball Berry model	m	-	7.0	5.7	8.0
Stomatal intercept parameter in Ball Berry model	b	mol m^{-2} s^{-1}	0.008	0.007	0.008
Stomatal sensitivity parameter	s_f	MPa^{-1}	6.5	6.5	6.5
Ψ_l at which half potential g_s is lost	Ψ_f	MPa	−1.3	−1.3	−1.3

Parenthetic numbers refer to references.
*Values for maize are obtained from the study of Drewry, et al. (2010a) (7).

1 Kromdijk J, et al. (2008) Bundle sheath leakiness and light limitation during c4 leaf and canopy co2 uptake. *Plant Physiol* 148:2144–2155.
2 Madakadze IC, et al. (1998) Leaf area development, light interception, and yield among switchgrass populations in a short-season area. *Crop Sci* 38:827–834.
3 Brutsaert W (1982) *Evaporation into the Atmosphere: Theory, History, and Applications*. (D. Reidel, London).
4 Farage PK, Blowers D, Long SP, Baker NR (2006) Low growth temperatures modify the efficiency of light use by photosystem II for CO_2 assimilation in leaves of two chilling-tolerant C4 species, Cyperus Longus l. and Miscanthus × Giganteus. *Plant Cell Environ* 29:720–728.
5 Campbell GS, Norman JM (1998) *An Introduction to Environmental Biophysics*. (Springer-Verlag, New York).
6 Clifton-Brown JC, Neilson B, Lewandowski I, Jones MB (2000) The modeled productivity of Miscanthus × Giganteus (Greef et deu) in Ireland. *Ind Crop Prod* 12:97–109.
7 Drewry D, et al. (2010a) Ecohydrological responses of dense canopies to environmental variability: 1. Interplay between vertical structure and photosynthetic pathway. *J Geophys Res* 115:G4, G04022.

Table S2. Change of total evapotranspiration (*ET*) and specific surface runoff (*R*) for the two cases shown in Fig. S6

Simulations	ΔET [mm]	ΔET [%]	ΔR [mm]	ΔR [%]
SEA—CTL	6.8	1.8	−0.7	1.7
MAX—CTL	12.2	3.2	−1.55	3.7

For CTL simulation, Total $ET = 380$ mm, and $R = 42$ mm (See Table 2 and Fig. 4 in the text)